PREDICTIONS FOR DYNAMIC SPECTRA AND SOURCE REGIONS OF TYPE II RADIO BURSTS IN THE INHOMOGENOUS CORONA AND SOLAR WIND

I. H. Cairns* and S.A. Knock*

Abstract

Shocks accelerate electrons and produce type II radio bursts in the inhomogeneous corona and solar wind. A recent semi-quantitative and macroscopic theory for type II bursts is reviewed and then extended to predict dynamic spectra and time-evolving source shapes (projected onto the plane of the sky) for multiple observers. Significant differences are found, suggesting that information on the 3-D source shape, motion, radio-loud hotspots and solar wind inhomogeneities should be obtained from dynamic spectra and direction-finding data provided by the STEREO spacecraft and near-Earth spacecraft like Wind.

1 Introduction

For over 50 years Type II solar radio bursts have been interpreted in terms of shocks that move through the solar corona, accelerate electrons, and produce radio emission near the local electron plasma frequency f_p and/or near $2f_p$ [Wild and McCready, 1950; Ginzburg and Zheleznyakov, 1958; Wild et al., 1963; Nelson and Melrose, 1985; Bastian et al., 1998; Robinson and Cairns, 1998; Cairns and Kaiser, 2002; Gopalswamy, 2004; Warmuth and Mann, 2005]. These shocks are usually associated with coronal mass ejections (CMEs) or flares and are then interpreted in terms of bow shocks driven ahead of CMEs and blast waves, respectively. At least some coronal shocks are expected to persist into the solar wind, raising the question as to whether interplanetary type II bursts exist. Cane et al. [1982] first observed these remotely. While interplanetary type IIs are now well accepted to be produced by CME-driven shocks, the relationships between coronal and interplanetary type IIs and between coronal type IIs, CMEs, flares, and blast waves remains controversial [Cane and Reames, 1988; Cliver et al., 1999; Reiner and Kaiser, 1999; Gopalswamy, 2000; Maia et al., 2000; Reiner et al., 2001; Cane and Erickson, 2005].

* *School of Physics, University of Sydney, Sydney, Australia*

The basic theoretical model for type II bursts involves formation of beams of electrons accelerated at the shock, growth of electrostatic Langmuir waves near f_p via an electron beam instability, and then the conversion of some Langmuir energy into radio emission near f_p and/or $2f_p$ via nonlinear processes [Ginsburg and Zhelezniakov, 1958; Nelson and Melrose, 1985; Bastian et al., 1998; Robinson and Cairns, 1998; Cairns and Kaiser, 2002]. It has proved difficult to detect locally active type II source regions, as evidenced by both electron acceleration and radio emission, although waves associated with shocks proved relatively easy to detect [Thejappa et al., 1995]. However, recently Bale et al. [1999] presented the first definitive identification and investigatation of the source region of an interplanetary type II burst, using a full suite of particle and field instruments. The data showed accelerated electrons streaming away from the shock, generating electrostatic Langmuir near f_p and radio emission near f_p and $2f_p$. Nevertheless, while these observations validate the basic theoretical model a large number of observational and theoretical issues remain [e.g., Bastian et al., 1998; Cairns and Kaiser, 2002; Cairns, 2004; Gopalswamy, 2004; Warmuth and Mann, 2005].

In the last 4 years a semi-quantitative, macroscopic theoretical model for type II emission has been developed [Knock et al., 2001, 2003a,b; Cairns et al., 2003; Knock and Cairns, 2005]. The goals of this paper are to: (1) present a brief review of the physics underlying the theory; (2) describe how the theory is implemented for a macroscopic shock moving through the inhomogenous corona and solar wind, including the effects of monotonic heliocentric variations of the plasma, shock and magnetic field parameters, as well as turbulence and prescribed structures like magnetic loops, magnetic clouds and corotating interaction regions (CIRs); (3) illustrate the theory's predictions for the radiation's dynamic spectrum and time-varying source characteristics for multiple observers, directly relevant to the upcoming STEREO mission; and (4) discuss the results and theory in connection with STEREO and future plans. The review of the theory and its implementation are described in Section 2, while the predictions relevant to STEREO are presented in Section 3. The discussion and conclusions are in Section 4.

2 Review of the theory

The macroscopic theory for type II bursts is constructed by calculating the radio emission associated with a local portion (ripple) of the global shock wave and then summing over ripples. Figure 1 illustrates the geometry of a ripple and its foreshock. For each ripple the theory involves four steps [Knock et al., 2001]: (1) Reflection and acceleration of electrons by the shock's magnetic mirror, using the Rankine-Hugoniot conditions to specify the magnetic jump, a model for the cross-shock potential [Kuncic et al., 2002a], and magnetic moment conservation and the cross-shock potential to describe the electron motion in the de Hoffman-Teller frame. (2) Prediction of the electron distribution function everywhere in the foreshock, using Liouville's theory and particle paths traced back to the shock and thence to the electron distribution function incident on the shock. (3) Estimation of the energy transfer from the electron beam into the Langmuir waves in steady-state, assuming that wave growth and associated quasilinear relaxation bring the system close to marginal stability, so that the energy transfer into the waves is given

by the convective derivative of the available beam free energy (including the quasilinear efficiency factor). (4) Estimation of the energy flux into fundamental and harmonic radio waves by multiplying the energy flux into the Langmuir waves by the known analytic conversion efficiencies between Langmuir waves and radiation for specific 3-wave nonlinear emission processes. The processes are the electrostatic decay $L \rightarrow L' + S$ of beam-driven Langmuir waves L into backscattered Langmuir waves L' and ion acoustic waves S, the fundamental emission process $L \rightarrow T(f_p) + S'$ which produces transverse radio waves near f_p and is stimulated by the S waves produced by ES decay, and the coalescence $L + L' \rightarrow T(2f_p)$ which produces radio waves near $2f_p$.

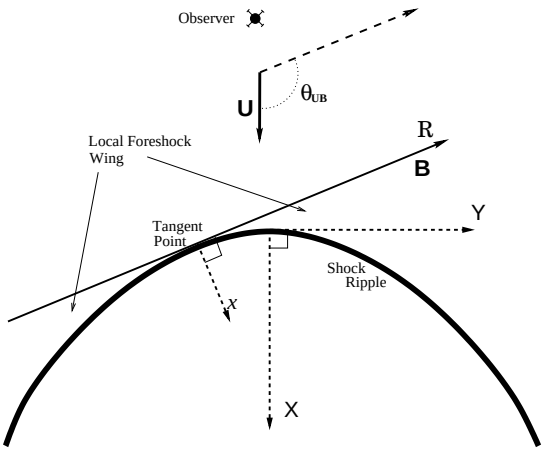

Figure 1: Schematic of a ripple in its rest frame, its foreshock regions, and definitions of the plasma flow velocity **U** *into the shock and the angle* θ_{UB} *between the upstream magnetic field vector* **B** *and* **U**.

The calculations for each step can be done analytically and combined with other steps, leading to predictions for the electron distribution functions and power flows into the radio waves as functions of position in the type II foreshock [Knock et al., 2001]. It is assumed that the incident electron distribution is a kappa distribution, thereby comprising a closely-Maxwellian core at thermal energies and an approximately power-law tail at high energies. Similar theoretical predictions exist for Earth's foreshock [Kuncic et al., 2002b]. Preliminary comparisons between the predicted and observed radio fluxes for one type II burst yield good agreement given uncertainties in the shock and plasma parameters [Knock et al., 2001]: the level of fundamental emission is underestimated by a factor of ≈ 10 while the harmonic level is overestimated by a factor ≈ 10.

The predicted radio flux depends sensitively on the shock and plasma parameters, plus observer location. For Figure 2 the plasma and shock parameters are appropriate to 1 AU: the paraboloidal ripple has a radius of curvature of 10^9 m at its nose, while the upstream plasma parameters are $T_e = 3T_i = 1.5 \times 10^5$ K, $n = 7$ cm^{-3}, $v_{sw} = 300$ km s^{-1}, the magnetic field has $B = 6$ nT and is oriented at an angle $\theta_{UB} = 85$ deg relative to the ripple's velocity vector, and the observer is located 10^9 m upstream from the ripple's nose along its velocity vector. Figure 2 shows that faster shocks are predicted to produce more intense type II bursts while sufficiently slow shocks should not produce observable radio emission [Knock et al., 2003a]. This is not inconsistent with observational findings

that faster (and larger) CMEs tend to produce brighter type II bursts [Cane et al., 1987; Cairns et al., 2003]. Not unexpectedly, the emission level decreases as the fraction of superthermal background solar wind electrons decreases (as the κ parameter increases from 2 to 5. Qualitatively, then, shocks moving through regions with enhanced populations of superthermal electrons (e.g., after previous flares or CMEs) are predicted to produce larger levels of radio emission for otherwise identical shock parameters. This is possibly relevant to "cannibalization" events and others in which a second CME moving through approximately the same spatial volume produces an observable radio burst whereas the first CME did not [e.g., Gopalswamy et al., 2001, 2002].

The fluxes in Figures 2 and 3 can be compared with the galactic background radiation, whose flux varies significantly with observing frequency [Dulk et al., 2001]: at 1 MHz, 300 kHz, and 100 kHz the flux is $\approx 10^{-19.3\pm0.1}$, $10^{-20.6\pm0.2}$, and $< 10^{-21.3}$ $\mathrm{Wm^{-2}Hz^{-1}}$, respectively. In comparison, those authors estimate the Wind spacecraft's noise level to be $\approx 10^{-21.4}$ $\mathrm{Wm^{-2}Hz^{-1}}$ in the range 100 - 400 kHz and $10^{-20.7}$ $\mathrm{Wm^{-2}Hz^{-1}}$ at 1 MHz. Evidently stringent conditions shock and plasma conditions (e.g., large U, high M_A, high n, large $\theta_{UB} \approx 90\,\mathrm{deg}$, large shocks, and/or large numbers of nonthermal electrons) and a sufficiently close observer is required for type II emission to be observable.

Figure 3 shows that shocks for which θ_{UB} is close to perpendicular are predicted to have higher levels of radio emission [Knock et al., 2003a], with quasi-parallel shocks predicted to have weak emission (especially for large κ). While this has been inferred remotely for some coronal type II bursts [e.g., Stewart and Magun, 1980], detailed testing of this prediction for *in situ* type II bursts has not yet been performed.

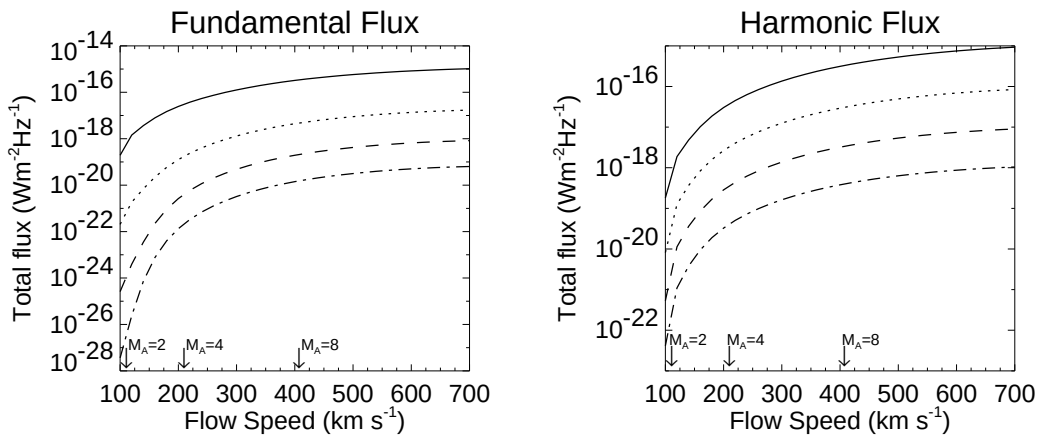

Figure 2: Predicted (a) fundamental and (b) harmonic flux for a ripple on a type II shock as a function of the shock speed $U = v_{sh} - v_{sw}$ relative to the upstream plasma flow [Knock et al., 2003a]. Each line is for a different κ parameter, ranging from 2 (solid) to 5 (dot-dash) as the relative fraction of nonthermal solar wind electrons decreases. The other shock and plasma parameters are listed in the text.

"Shadowing" and "multiple beam" effects by neighboring ripples will affect particle paths in the foreshock, thereby modifying the predicted electron distributions and levels of Langmuir and radio waves. Accordingly it might be wondered whether having multiple

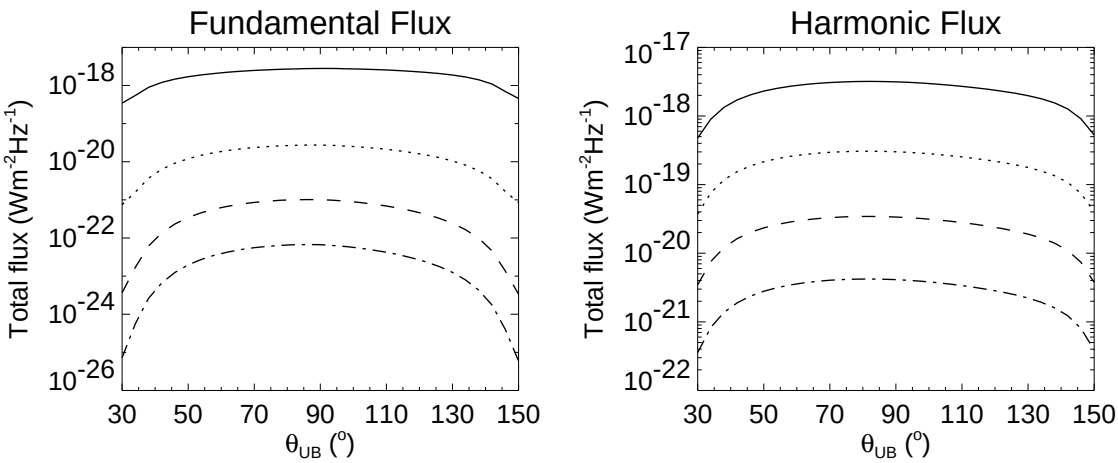

Figure 3: Predicted (a) fundamental and (b) harmonic flux for a ripple with $U = 300$ km s^{-1} as a function of the angle θ_{UB} between the magnetic field vector and the ripple's relative velocity vector [Knock et al., 2003a]. The line style identifies the value of κ in the same way as in Figure 2. The shock and plasma parameters other than U and θ_{UB} are as for Figure 2.

simultaneous ripples on the macroscopic shock will qualitatively affect the overall flux and dynamic spectrum predicted. Importantly, calculations in Figure 4(Left) show that ripples are independent to a good approximation [Knock et al., 2003b]: the flux predicted for multiple realizations of the same seven 2-D ripples randomly located within a spatial interval, when multiple beam and shadowing effects are included, is within $\approx 30\%$ of that predicted assuming the ripples to be independent. Accordingly, in the calculations below ripples are assumed to be independent, greatly simplifying the calculations and length of the simulation runs.

Implementation of the macroscopic theory requires specification of (1) the time-evolving radius of curvature, 3-D location, and average velocity of the macroscopic parabolic shock, (2) the properties of the inhomogeneous solar wind plasma, and (3) the properties of ripples on the macroscopic shock [Knock et al., 2003b; Knock and Cairns, 2004]. The solar wind properties are assumed to be inhomogeneous, both on macroscopic scales and on the scale of a ripple. The macroscopic variations are two-fold. The first is conventional, corresponding to standard variations with heliocentric distance R: the plasma density n_{sw} varies as R^{-2} once beyond a few solar radii and has $n_{sw} = 7$ cm^{-3} at 1 AU , the solar wind velocity $\mathbf{v}_{sw}$ is radially directed with approximately constant magnitude $v_{sw} = 400$ km s^{-1}, the vector magnetic field obeys the 2-D Parker solution with $B = 5$ nT and an angle of 45 deg at 1 AU, and the electron and ion temperatures are power-law functions of R. The second, superposed on the heliocentric variations, are large-scale solar wind structures like corotating interacting regions (CIRs) and CME-associated magnetic clouds. See Knock et al. [2003b] and Knock and Cairns [2005] for more details on these macroscopic variations.

Turning now to the ripples, these are assumed to be paraboloidal perturbations that evolve (that means to appear and disappear) on a time scale R_c/V_A, where R_c is the ripple's radius of curvature and V_A is the Alfven speed. They are assumed to vary with R, with R_c Gaussian distributed around the decorrelation length of the magnetic field.

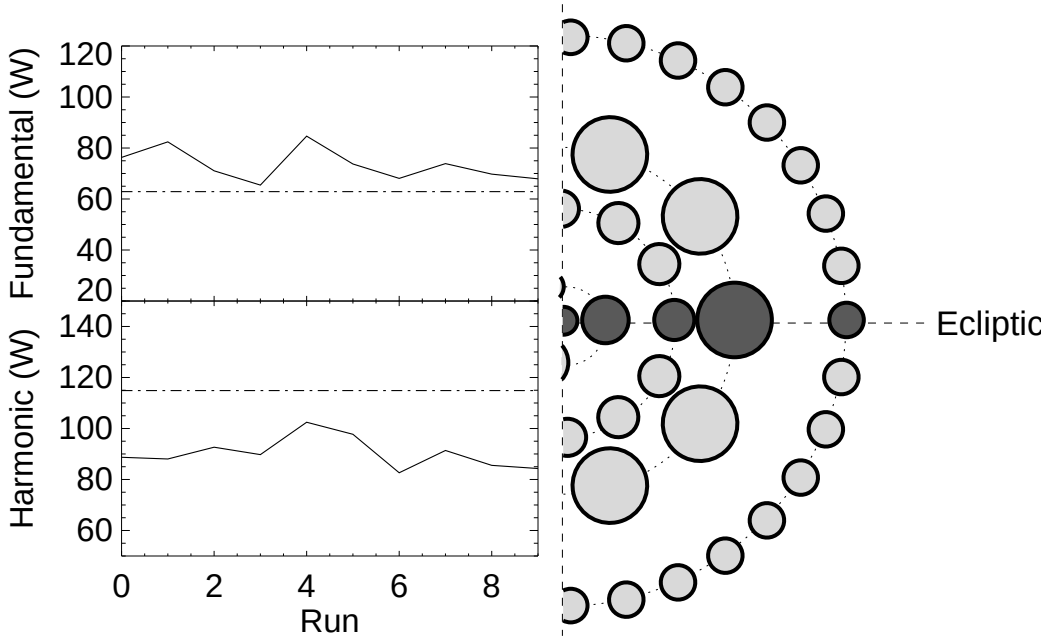

Figure 4: (Left) Fundamental and harmonic flux predicted for multiple realizations of 7 randomly-located ripples, including multiple beam and shadowing effects on the electron distribution functions (solid line), compared with the summed flux from the same 7 ripples when calculated in isolation (dashed line) [Knock et al., 2003b]. (Right) Illustration of how ripples are packed with half-hemispherical symmetry onto the macroscopic shock [Knock and Cairns, 2005]. See text for more details.

Computational limitations currently prevent the ripples being randomly packed onto the macroscopic shock and the contribution to the dynamic spectrum being calculated exactly. Instead, the ripples are closely packed with modified azimuthal symmetry about the Sunwards direction, as shown in Figure 4(Right): looking Sunwards with the ecliptic plane horizontal, the eastern and western hemispheres of the macroscopic shock are packed independently and in an azimuthally symmetric fashion with ripples. The ripples are closely packed, with their radius of curvature equal to their separation distance, and their properties are chosen in the ecliptic plane: to include solar wind variability on ripple scales, the solar wind density, velocity, temperatures, and magnetic field are perturbed with Gaussian-distributed fluctuations about the macroscopic model predictions for the ecliptic plane. Then the radiation produced by a given ripple in the ecliptic plane is calculated, assuming no interactions with neighboring ripples. Despite the azimuthal symmetries assumed for the ripples due to computational limitations, with every ripple at a given polar angle identical for the eastern and western hemisphere, the falloff in the radiation flux with distance between the observer and each ripple is calculated exactly along straight line propagation paths. Moreover, if the plasma frequency along the path to the observer for a given ripple exceeds the radiation frequency, then the radiation is "blocked" and is not detected by the observer. As discussed more below, isotropic emission patterns are assumed and scattering is not included.

3 Dynamic spectrum and direction-finding results

Figures 5 and 6 show dynamic spectra for the foregoing macroscopic shock theory, details of the solar wind inhomogeneities for the calculated situation, and the time-evolving source shapes (projected onto the plane of the sky) for several observers. Specifically, they are calculated for a macroscopic shock directed exactly at the Earth and observed by two observers (see Figures 5 and 6): one well off to the western side of the Earth at solar-ecliptic coordinates $(100, -100, 0)$ Gm, potentially the STEREO-B spacecraft, and the second close to the Earth at location $(148, 1, 0)$ Gm, for instance the Wind spacecraft. In addition, the Figures illustrate the solar wind inhomogeneneities assumed and snapshots of the shock's position and the predicted radio source. This latter calculation corresponds to the direction finding information an ideal observing instrument would have available. The extraction of source information on type II bursts from the dynamic spectra and direction-finding data for two or more widely separated observers is one major goal of the upcoming STEREO mission (presently scheduled for launch in April 2006).

The inhomogeneous solar wind context in the ecliptic plane is shown in the lower left panel for each Figure, using the electron temperature T_e, as well as the time-varying location of the macroscopic shock (white parabola). Similar panels are shown by Knock and Cairns [2005]. Visible are, first, the monotonic decrease in T_e with heliocentric distance (note the slow change in colour from left to right), second, two CIRs (the expanding fan shapes) and one magnetic cloud (the circular depresssion in T_e), and third the random variations in T_e on ripple scales.

Clear differences are visible in the dynamic spectra (top panels) for the two observers. These are due to the different relative distances between observers and elements (ripples) of the macroscopic source, plus frequency blocking effects. Thus, the theory predicts that dynamic spectra from multiple observers contain information on relative source-observer locations and the inhomogeneous plasma environment. Direction finding, however, may be required to usefully constrain this information. Moreover, other physics related to scattering and directivity patterns may need to be added: while angular broadening and time delays due to scattering by density irregularities are likely to smooth fine structure in the dynamic spectrum, non-isotropic intrinsic directivity patterns for either radiation component would further modify the predictions for different observers.

It is crucial to notice that some features in the dynamic spectra relate specifically to the interaction of the shock with macroscopic solar wind features. For instance, the intense (red) short-lived features at constant frequency at the times of the vertical and parabolic white lines in the top and leftmost bottom panel, respectively, correspond to the macroscopic shock crossing a magnetic cloud while the multiple long-lived curving features relate to the shock's interaction with CIRs [Knock and Cairns, 2005]. Previously Reiner et al. [2001] have observed spectral intensifications associated with a type II shock crossing a CIR, while Gopalswamy et al. [2001, 2002] have interpreted some coronal radio emissions in terms of a CME-associated shock catching up with an earlier CME event and "cannibalizing" it. These interactions can be used to further develop and test the theory, since the predicted emission depends sensitively on the plasma and shock properties (e.g., Figures 2, 3, 5 and 6).

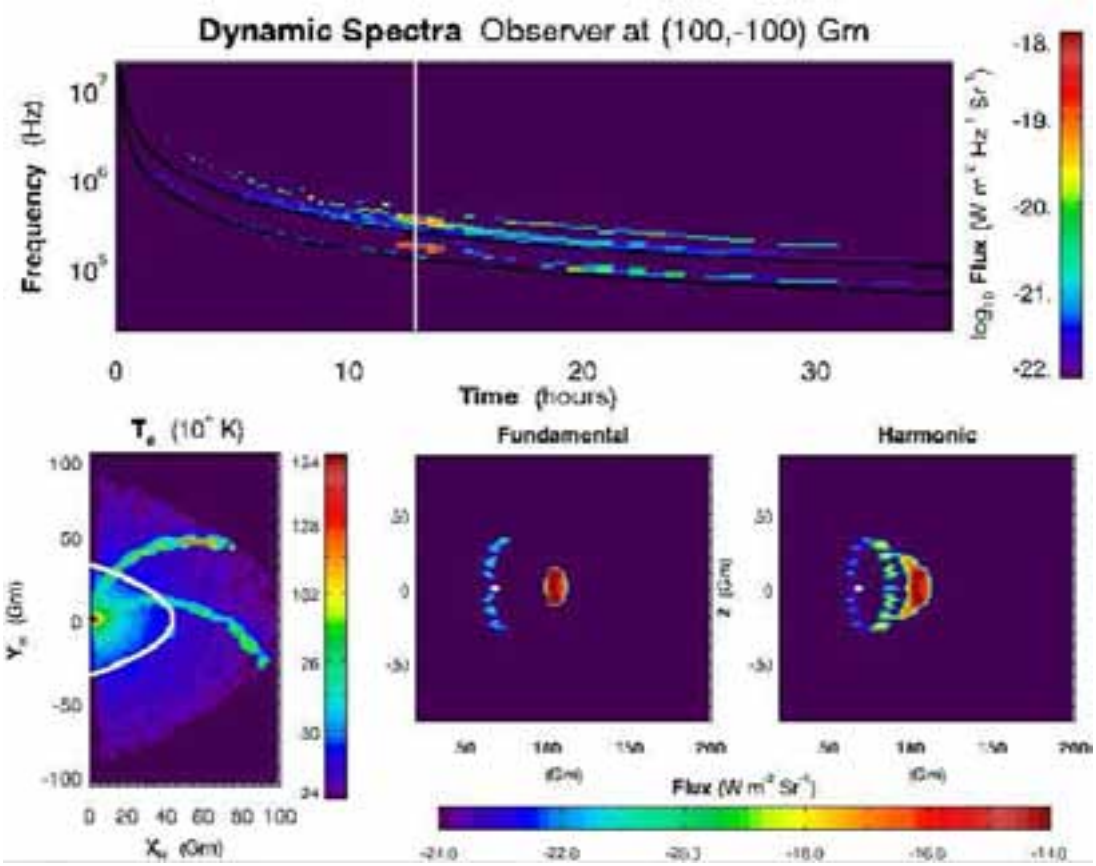

Figure 5: (Top) Predicted dynamic spectrum, (bottom left) model electron temperature as a function of position in the ecliptic plane, and (bottom center and right) snapshots of the predicted source locations of fundamental and harmonic radiation, projected into the plane of the sky, for an observer at location $(100, -100, 0)$ *Gm in solar-ecliptic coordinates. The snapshots are taken for the shock location and time shown by the parabolic and vertical white lines, respectively, in the leftmost and top panels.*

The two rightmost bottom panels of Figures 5 and 6 show the source location, projected onto the plane of the sky, for fundamental and harmonic radiation at the time when the macroscopic shock is crossing the first magnetic cloud (vertical and parabolic white lines in the Figures' top and leftmost bottom panels). Emission from individual ripples is clearly visible. In addition, Figure 5, for the western observer, shows the 3-D macroscopic source shape to be a paraboloid (e.g., a shuttlecock) that is not seen exactly perpendicular to the direction of the source centroid's motion (e.g., ripples at a constant polar angle but not identical azimuthal angles do not project onto a straight line). The theory's predictions therefore suggest that direction-finding with STEREO and other spacecraft might permit the source's 3-D shape, including asymmetries, and direction of motion to be inferred remotely. If achieved observationally, this would be extremely useful in predicting the arrival or not of space weather events at Earth.

The situation for the head-on observer is presented in Figure 6. Complementary information on the shock's 3-D structure from the western observer is evident. In particular, the

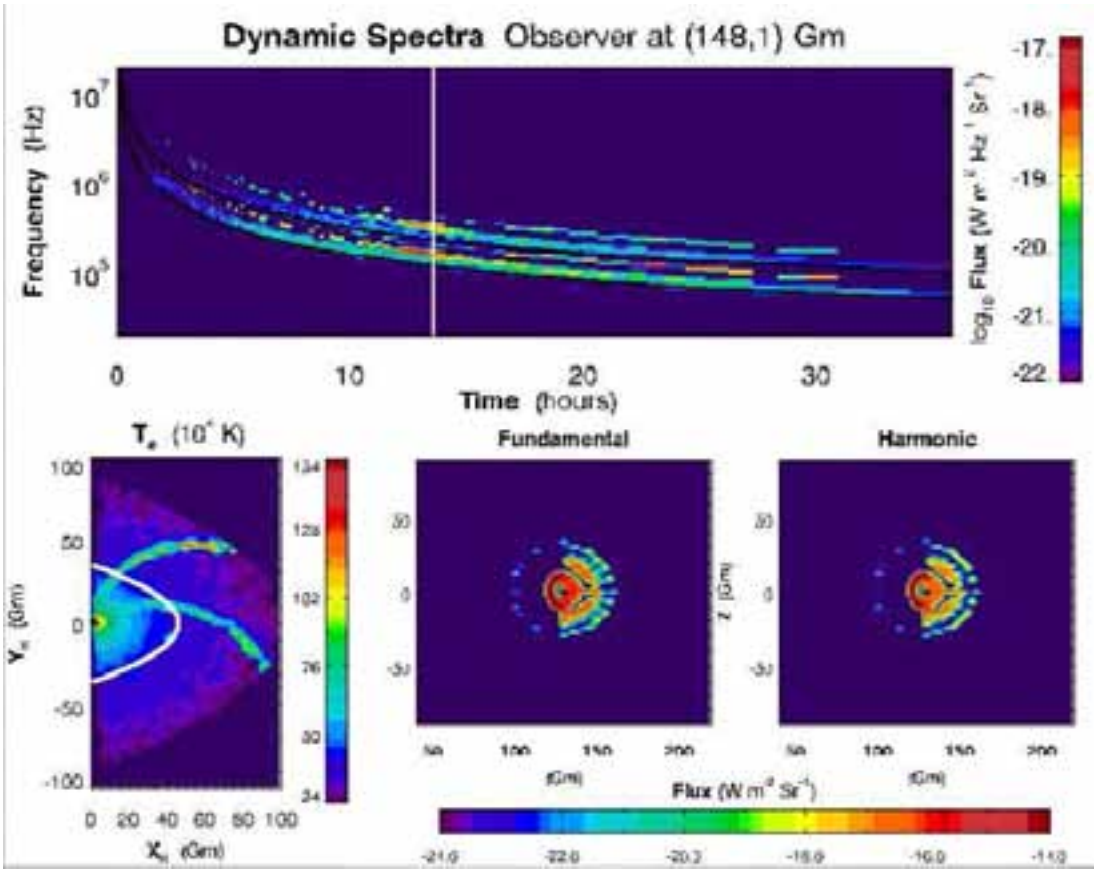

Figure 6: Dynamic spectrum, electron temperature, and snapshots of the source location in Figure 4's format for an observer very close to the Earth, at location $(148, 1, 0)$ *Gm.*

azimuthal ripple-packing symmetries assumed in this theoretical implementation is clear. Despite the symmetry being unrealistic for a real type II shock it does elucidate the role of the macroscopic magnetic field direction: note that the eastern (right-side) ripples are on average much more intense than the western ripples, consistent with the angles between the macroscopic shock normal and Parker spiral field being closest to 90 deg and so Figure 3 predicting larger emission for otherwise identical ripple parameters. Put another way, the eastern hemispheric of the shock is quasi-perpendicular while the western hemisphere is quasi-parallel, so that the dominant emission is predicted from the eastern hemisphere.

4 Discussion and Summary

A semi-quantitative macroscopic theory thus exists for type II radio bursts in the corona and solar wind, based on relatively conservative physics: magnetic mirror reflection of electrons, beam formation by time-of-flight, energy flow into the Langmuir waves given time-steady quasilinear relaxation, specific nonlinear Langmuir wave processes, and ripples on the macroscopic shock surface with scales commensurate with the decorrelation length of the magnetic field. The theory has been implemented numerically to yield pre-

dictions for the dynamic spectra and 3-D source shape of a shock propagating through the inhomogeneous corona solar wind, including heliocentric variations in the plasma and shock parameters, macroscopic structures like CIRs and magnetic clouds, and random variations on a ripple scale. Enhanced emission associated with the shock interacting with macroscopic structures is predicted, in manners not inconsistent with recent observations. The new results here include predictions for the dynamic spectra and time-varying projected source shape (on the plane of the sky) for multiple observers which contain information on the 3-D shock shape, radio-loud hotspots thereon, and inhomogeneities in the solar wind. The predictions suggest that information on the 3-D source shape, motion, and radio-loud hotspots should be accessible from dynamic spectra and direction-finding observations from the two STEREO spacecraft and near-Earth assets like Wind.

Further analysis is necessary to see whether the observing modes and properties of the STEREO radio and plasma wave instrument (J.-L. Bougeret, principal investigator, http://www-lep.gsfc.nasa.gov/swaves/swaves.html) will actually permit extraction of the above source information from the theoretically predicted dynamic spectra and direction-finding information. On the theoretical side, developing more realistic predictions will involve reducing the model packing symmetries assumed, better mimicking solar wind structures like CIRs and magnetic clouds, and including the effects of anisotropic directivty patterns and scattering. Moreover, it would be ideal if the theory could be extended to follow the MHD evolution of a shock through the inhomogeneous corona and then to predict the dynamic spectrum and projected time-varying source properties. Finally, more detailed comparisons between observations and predictions for the dynamic spectra, radiation levels, Langmuir wave characteristics, and accelerated electrons are necessary to test the theory and refine it as required.

References

Bale, S. D., M. J. Reiner, J.-L. Bougeret, M. L. Kaiser, S. Krucker, and D. E. Larson, The source region of an interplanetary type II burst, *Geophys. Res. Lett.*, **26**, 1573–1576, 1999.

Bastian, T. S., A. O. Benz, and D. E. Gary, Radio emission from Solar flares, *Ann. Rev. Astron. Astrophys.*, **36**, 131–188, 1998.

Cairns, I. H., Solar, interplanetary, planetary, and related extra-solar system science for LOFAR, *Planet. Space Sci.*, **52**, 1423–1434, 2004.

Cairns, I.H., and M.L. Kaiser, Solar system radio emissions, in "The Review of Radio Science 1999 – 2002, Ed. W. Russ Stone, p. 749–774, IEEE Press, 2002.

Cairns, I. H., S. A. Knock, P. A. Robinson, and Z. Kuncic, Type II solar radio bursts: theory and space weather implications, *Space Sci. Rev.*, **107**, 27–34, 2003.

Cane, H. V., and D. V. Reames, Soft X-ray emissions, meter-wavelength radio bursts, and particle acceleration in solar flares, *Astrophys. J.*, **325**, 895–900, 1988.

Cane, H. V., and W. A. Erickson, Solar type II radio bursts and IP type II events, *Astrophys. J.*, **623**, 1180–1194, 2005.

Cane, H. V., N. R. Sheely Jr., and R. A. Howard, Energetic interplanetary shocks, radio emission, and coronal mass ejections, *J. Geophys. Res.*, **92**, 9869–9874, 1987.

Cane, H. V., R. G. Stone, G. Fainberg, J. L. Steinberg, and S. Hoang, Type II Solar radio events observed in the interplanetary medium, *Solar Phys.*, **78,** 187–198, 1982.

Cliver, E. W., D. F. Webb, and R. A. Howard, On the origin of solar metric type II bursts, *Sol. Phys.*, **187**, 89–114, 1999.

Dulk, G. A., W. C. Erickson, R. Manning, and J.-L. Bougeret, Calibration of low-frequency radio telescopes using the galactic background radiation, *Astron. Astrophys.*, **365**, 294–300, 2001.

Ginsburg, V. L., V. V. Zhelezniakov, On the possible mechanisms of sporadic solar radio emission, *Sov. astron. zhurn.*, **35**, 694, 1958.

Gopalswamy, N., Recent advances in the long-wavelength radio physics of the Sun, *Planet. Space Sci.*, **52**, 1399–1413, 2004.

Gopalswamy, N., S. Yashiro, M. L. Kaiser, R. A. Howard, and J.-L. Bougeret, Radio signatures of coronal mass ejection interaction: coronal mass ejection cannibalism?, *Astrophys. J. (Letters)*, **548**, L91–L94, 2001.

Gopalswamy, N., S. Yashiro, M. L. Kaiser, R. A. Howard, and J.-L. Bougeret, Interplanetary radio emission due to interaction between two coronal mass ejections, *Geophys. Res. Lett.*, **29**, 106–109, 2002.

Knock, S., I.H. Cairns, P.A. Robinson, and Z. Kuncic, Theory of type II solar radio emission from the foreshock region of an interplanetary shock, *J. Geophys. Res.*, **106**, 25 041–25 052, 2001.

Knock, S.A., I.H. Cairns, P.A. Robinson, and Z. Kuncic, Theoretically predicted properties of type II radio emission from an interplanetary foreshock, *J. Geophys. Res.*, **108(A3)**, doi:10.1029/2002JA009508, SSH 6-1, 2003a.

Knock, S.A., I.H. Cairns, and P.A. Robinson, Type II radio emission predictions: Multiple shock ripples and dynamic spectra, *J. Geophys. Res.*, **108(A10)**, SSH 2-1, 2003b.

Kuncic, Z., I. H. Cairns, and S. A. Knock, Analytic model for the electrostatic potential jump across collisionless shocks, with application to Earth's bow shock, *J. Geophys. Res.*, **107(8)**, doi:10.1029 2001JA000250, SSH 11-1, 2002a.

Kuncic, Z., I. H. Cairns, S. A. Knock, and P. A. Robinson, A quantitative theory for terrestrial foreshock radio emissions, *Geophys. Res. Lett.*, 29(8), doi:10.1029 2001GL024524, 2-1, 2002b.

Kuncic, Z., I.H. Cairns, and S.A. Knock, A quantitative model for terrestrial foreshock radio emissions I: Predicted properties, *J. Geophys. Res.*, **109(A3)**, A02108 (1-15), doi:10.1029/2003JA010125, 2004.

Maia, D., M. Pick, A. Vourlidas, R.A. Howard, Development of coronal mass ejections: radio shock signatures, *Astrophys. J.*, **528**, L49-L51, 2000.

Nelson, G. S., and D. Melrose, *Solar Radiophysics*, edited by D. J. McLean, and N. R. Labrum, p. 333, Cambridge University Press, Cambridge, 1985.

Reiner, M. J., and M. L. Kaiser, High-frequency type II radio emissions associated with shocks driven by CMEs, *J. Geophys. Res.*, **104**, 16 979–16 992, 1999.

Reiner, M. J., M. L. Kaiser, and J.-L. Bougeret, Radio signatures of the origin and propagation of coronal mass ejections from the solar corona and interplanetary medium, *J. Geophys. Res.*, **106**, 29 989–30 000, 2001.

Robinson, P. A., and I. H. Cairns, Theory of type III and type II Solar radio emission, in *Radio Astronomy at Long Wavelengths*, eds. R. Stone, E. Weiler, and M. Goldstein, Geophysical Monograph 119, American Geophysical Union, 37–45, 2000.

Stewart, R. T., and A. Magun, Radio evidence for electron acceleration by transverse shock waves in herringbone type II solar radio bursts, *Proc. Astron. Soc. Aust.*, **4(1)**, 53–55, 1980.

Thejappa, G., D. G. Wentzel, R. J. MacDowall, and R. G. Stone, Unusual wave phenomena near interplanetary shocks at high latitudes, *Geophys. Res. Lett.,* **22,** 3421–3424, 1995.

Warmuth, A., and G. Mann, The application of radio diagnostics to the study of the solar drivers of space weather, in *Space Weather*, eds K. Scherer, H. Fichtner, B. Heber, and U. Mall, Lect. Notes Phys. 656, Springer, 51–70, 2005.

Wild, J. P., and L. L. McCready, Observations of the spectrum of high–intensity Solar radiation at meter wavelengths - I. The apparatus and spectral types of Solar bursts observed, *Austr. J. Sci. Res., Ser. A*, **3**, 387–398, 1950.

Wild, J. P., S. F. Smerd, and A. Weiss, Solar bursts, *Ann. Rev. Astron. Astrophys.*, **1**, 291–366, 1963.